Monolithic fabrication of Rotman lenses

Leonard Hall[a], Hedley Hansen[b] and Derek Abbott[a]

[a]Centre for Biomedical Engineering and
Department of Electrical and Electronic Engineering
Adelaide University, SA 5005, Australia
E-mail: lthall@eleceng.adelaide.edu.au

[b]DSTO
EWD, PO Box 1500, Salisbury SA 5108
E-mail: hedley.hansen@dsto.defence.gov.au

ABSTRACT

Rotman lenses have the potential to solve many problems associated with high frequency antenna arrays. Offering compact, rugged and reliable means of forming multi-beam, staring array sensing arrangements, these lenses may prove very useful if robust solutions to some important problems are to be found. This paper presents the performance of a Rotman lens design and discusses the challenges associated with the design of these lenses.

Keywords: Microstrip, Rotman lens, beam-forming

1. INTRODUCTION

Sensors operating in the mm-wave (20-100 GHz) band have better poor weather performance than those operating at smaller IR and visible wavelengths. Naturally occurring 37 and 94 GHz radiation propagates through cloud, smoke, fog and other such aerosols, as seen by the attenuation curve in Fig. 1. Millimeter wave systems provide better spatial resolution (and target discrimination) than systems operating at centimeter and meter wavelengths and comprise of very compact, low weight and physically small antennas. These properties make millimeter wave sensors an attractive option in a variety of defence, security-related and civilian remote sensing applications.

Beamforming mm-wave antennas have numerous applications including radar,[1] communication[2,3] and biomedical systems,[4,5] synthetic vision schemes and automobile collision-avoidance systems.[6–13] The Rotman lens described here is a prototype lens used in the development of a passive mm-wave collision avoidance system.[7,14–21]

This paper describes the development of a Rotman lens-based antenna array,[22] to be operated at 15 GHz. The design and simulated responses are presented. A characteristic of this design is that it is to be monolithically fabricated so that it provides a low-cost testing platform of the design for further versions at higher frequencies eg. 37 and 94 GHz.

2. THE SENSOR WITH SPECIFICATIONS FOR INTEGRATED DESIGN

The radiometric sensor described below employs a beamforming Rotman lens which allows simultaneous scanning or staring array sensing over a large field-of-view. The Rotman lens arrangement consists of a parallel plate region with beam ports and array ports distributed along opposite contours. The central beamport provides equal path lengths to each array element. An offset beam produces a path length and hence a phase gradient along an array giving a steered beam. A Rotman lens approach promises the advantages of inherent wide bandwidth, the possibility of full integration with detection circuitry at mm-wave frequencies.

The initial design that is being considered is a 15 GHz lens for steering nine beams with a 40° scan angle. This provides a simple prototype to enable rapid development of the skills required for the design's manufacture at affordable cost. In addition in this design, the half-wavelength separation of beamports is achievable and therefore spillover losses can be kept low.

The lens and the feeds are to be implemented using microstrip fed by patch antenna elements. A schematic of the system is shown in Fig. 2(a). This architecture provides a compact structure that is planar and is compatible with monolithic fabrication. The theoretical radiation pattern of this system is in Fig. 2(b), showing a scan coverage of 40° for beams of 10° beamwidth and sidelobes levels of -15 dB.

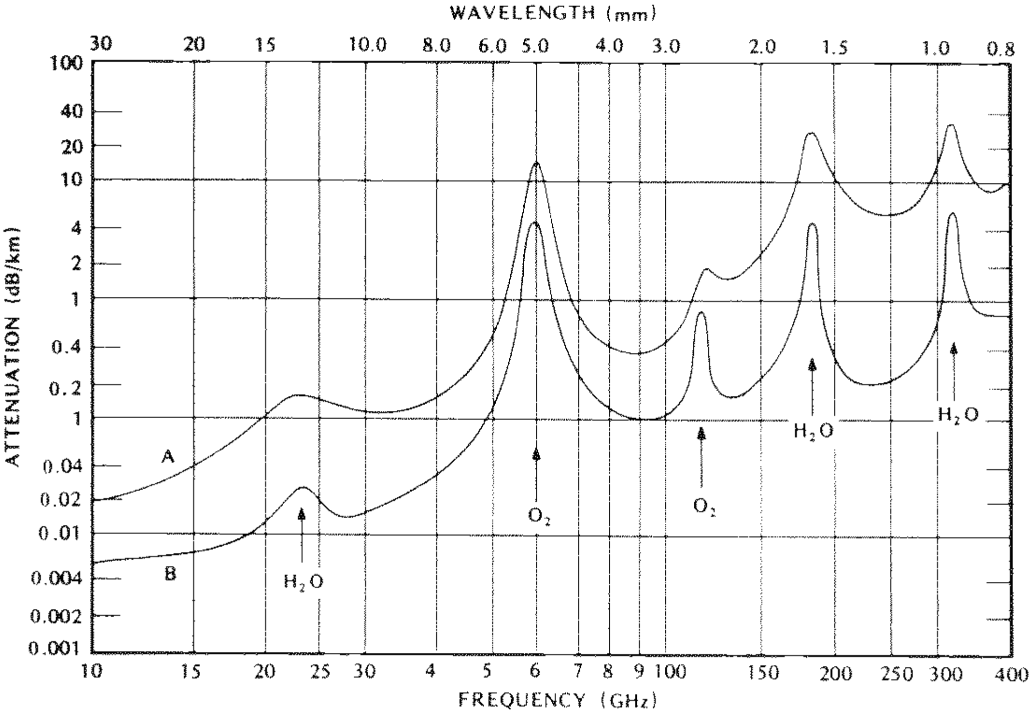

Fig. 1. The one way attenuation of electromagnetic radiation in the troposphere[23]

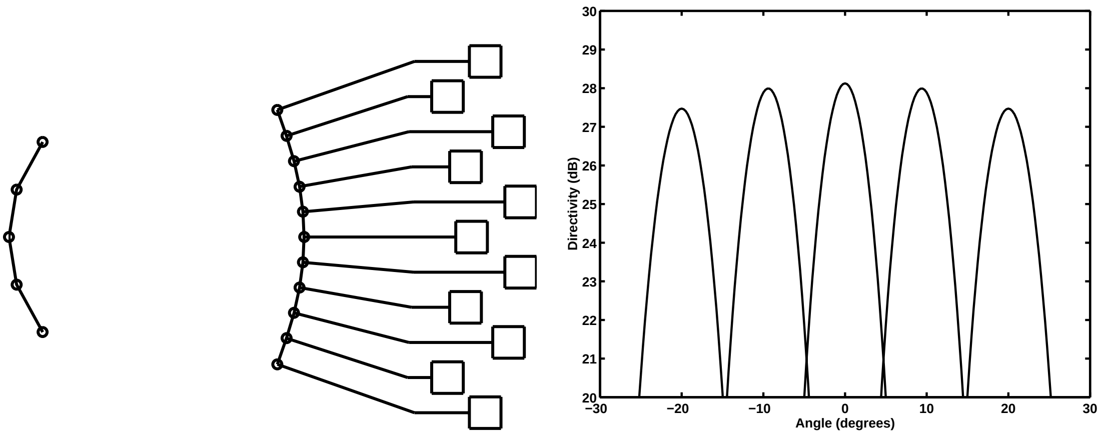

(a) Layout utilising Patch antenna

(b) Theoretical radiation pattern

Fig. 2. Basic Rotman Lens Design

3. SIMULATION

In order to design the lens a process utilising three levels of simulation is employed. This allows the performance of the device to be adequately predicted before prototype designs are manufactured.

Level one simulation involves the numerical optimisation of the Rotman geometry using ideal models.[24] The lens is modelled using geometric optics. No coupling between input and output ports is considered, with all ports matched and reflections and attenuation ignored.

Level two simulation addresses the non-ideal effects of the microstrip and how adopting various antenna element options affect performance.[25] Level two simulations include optimising the bandwidth performance of the lens.

Level three simulation calculates the impedance at each of the beam ports, array ports and dummy ports, so that effective matching networks can be designed. The various antenna patterns associated with each beam port are therefore provided.

3.1. Level 1 and 2, Ideal and Non-Ideal Modelling

Scattering matrices have been used exclusively throughout the simulation. Three scattering matrices have been generated, S_B accounting for the Rotman lens body, S_W for the path delays between antenna elements and associated antenna ports on the inner lens contour and S_A for the phase delays between incoming rays onto the antenna array. Combining these matrices has provided the output at each port due to any given incident wave.

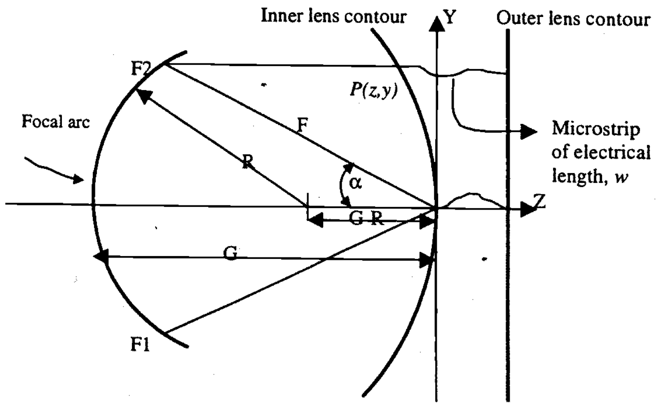

Fig. 3. Rotman Lens Topology[22]

The design of the lens or matrix S_A is governed by the Rotman-Turner design equations. These expressions are given as follows, using the variables defined in Fig.3:

$$\begin{aligned} y &= \frac{Y}{F} \\ z &= \frac{Z}{F} \\ n &= \frac{N}{F} \\ g &= \frac{G}{F} \\ w &= \frac{W - W_o}{F} \\ a &= \cos(\alpha) \\ b &= \sin(\alpha) \\ 0 &= Aw^2 + Bw + C \end{aligned}$$

$$
\begin{aligned}
A &= 1 - \frac{(g-1)^2}{(g-a)^2} - n^2 \\
B &= -2g - n^2 b^2 \frac{g-1}{(g-a)^2} + 2g\frac{g-1}{g-a} \\
C &= -\frac{n^4 b^4}{4(g-a)^2} + g\frac{n^4 b^4}{g-a} - n^2 \\
R &= \frac{(Fa-G)^2 + F^2 b^2}{2(G-Fa)}
\end{aligned}
$$

where $P(Z,Y)$ is the position of the antenna ports, $P(\theta,R)$ is the position of the beam ports N is the position of each antenna in the horizontal plain and W is the added delay length between antenna and lens.

Fig. 2(a) showed the layout of the eleven antenna element, five beam port configuration under consideration where the opposite contours are clearly shown. The design frequency of the simulations that follow is 15 GHz. A normalised focal length ratio of g = 1.06 is used with the off-axis focal point angle of 20°. Fig. 4(a) shows the desired phase delays between antenna elements and their corresponding antenna ports. Fig. 4(b) displays the maximum phase error versus angle. For the three focal points the phase error is negligible and *between* these points the phase error remains $< 0.7°$. Fig. 5(a) then displays the center beam of the idealised eleven-beam radiation pattern.

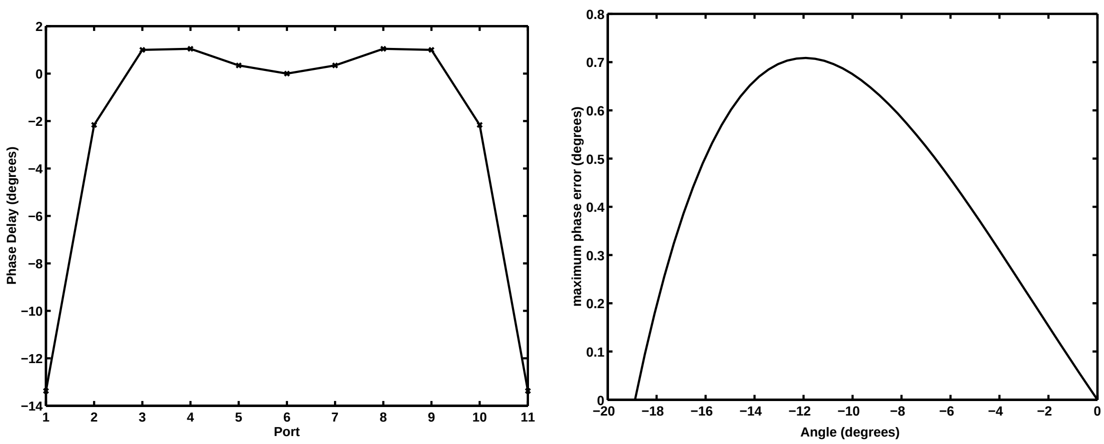

(a) Path delay versus antenna element

(b) Phase error versus beam angle

Fig. 4. Basic Rotman Lens Design

The adverse affect of using non-ideal antenna elements within a microstrip lens structure has been accounted for. Using appropriate S_A and S_W matrices, the losses in the system increase and have a minor effect in shaping the beam radiation patterns.[26]

3.2. Implementation of Design

Using this model, the effects of various design changes have been examined. Fig. 5(b) shows the design with quarter wave matching networks between the lens and microstrip lines. Earlier designs employed a dipole antenna array[13,19,20] due to the possibility of stacking 1-D arrays to form a 2-D coverage. Fig. 5(b) shows patch antenna elements are adopted. Patch antennas have a number of inherent advantages over other antenna designs. They are mounted and matched to the microstrip by a $\lambda/4$ impedance transformer with ease, and they have low levels of cross-coupling. Patch antennas radiate perpendicularly to the surface they are mounted on and this allows them to be moved in the X direction, without disturbing their performance in the Z-Y plane. This feature has been exploited in the design because it allowed greater freedom in accommodating simple microstrip architectures (eg., straight lines) which avoid electromagnetic discontinuities. Moreover, it also allowed an array configuration to be adopted where mutual coupling was reduced to insignificant levels. It should be noted that an important aspect of this patch antenna array structure is the reduction in beam-width in the Z-X plane. This is displayed in Fig. 5(c), where a narrowing of the beam and the lobes on both sides of the main beam is shown.

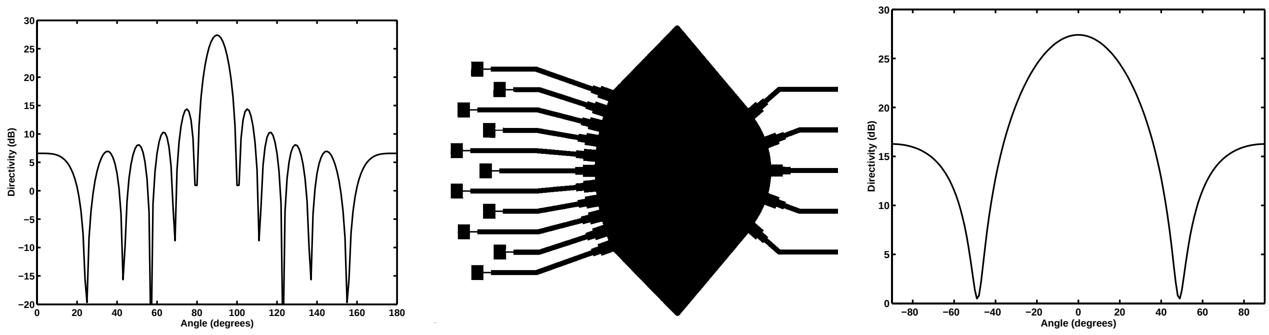

(a) Sidelobe Level (b) Final Layout (c) Beam pattern 90° to scan

Fig. 5. Level 2 Simulation Results

To achieve low side-lobe levels reflections within the body of the Rotman lens must be minimised. In this design this has been done by tapering the sides of the lens out to a point. Waves must be reflected multiple times before encountering a port, in doing so, the wave is substantially attenuated.

3.3. Level 3 - Electromagnetic Modelling

Electromagnetic simulation provides the link between the design, and the final Rotman lens realisation. This initially involves calculating the impedances of the beam, and array ports around the body of the lens. Networks then match each of the ports to a 50 Ω line. For narrow bandwidths a quarter wave impedance transformer is adequate, however, for broadband performance, more complicated networks must be used.[27,28] In this design the ports have not been individually matched, instead the impedance has been reduced to 25 Ω which roughly corresponds to the impedance looking into the body of the lens. The width of the line connecting the body of the lens to the 50 Ω line, is designed so that only first order modes are allowed to propagate. Higher order modes are then confined to the body of the lens.

The simulated beam pattern associated with the lens comprising matching networks is shown in Fig. 6(a) and 6(b). Sidelobes of -7 dB at 0° beam port, increasing to -6 dB at the 20° beam ports, are disappointing.

4. MEASURED RESULTS

The transition from design to prototype generally introduces a number of new effects that are difficult to account for in design. The prototype has a finite ground plain, the edge of which is close to the array of patch antennas and the corners at either edge of the design. Due to a problem in the layout software, all corners between edges not parallel with the edge of the board, have been rounded. The patch antennas are unaffected however the quarter wave matching networks have been altered.

Despite the manufacturing faults, the lens performs better than the electromagnetic simulations predict. Fig. 7(a) shows a maximum gain of 17.5 dB and sidelobes of -15 dB for the 0° port and Fig. 7(b) shows a maximum gain of 10 dB and sidelobes of -8 dB for the 20° port. This compares very well with the values of 14.5 dB maximum gain and -8 dB sidelobes for the 0° port and 14 dB maximum gain and -7 dB sidelobes for the 20° port, predicted by the electromagnetic simulation Fig. 6(a) and 6(b). The increase in gain is due to the reduction in sidelobe strength, however, the position of the sidelobes are consistent. This may be caused by the finite ground plane reducing reflections from the sidewalls of the lens.

S_{11} of 0° and 20° ports are shown in Fig. 8(a) and 8(b) respectively. There is a substantial difference between the 0° port that has not been altered in manufacture and the 20° which has. However, this discrepancy may also be caused by the different position on the Rotman lens. Although not ideal, S_{11} performance of the ports is acceptable.

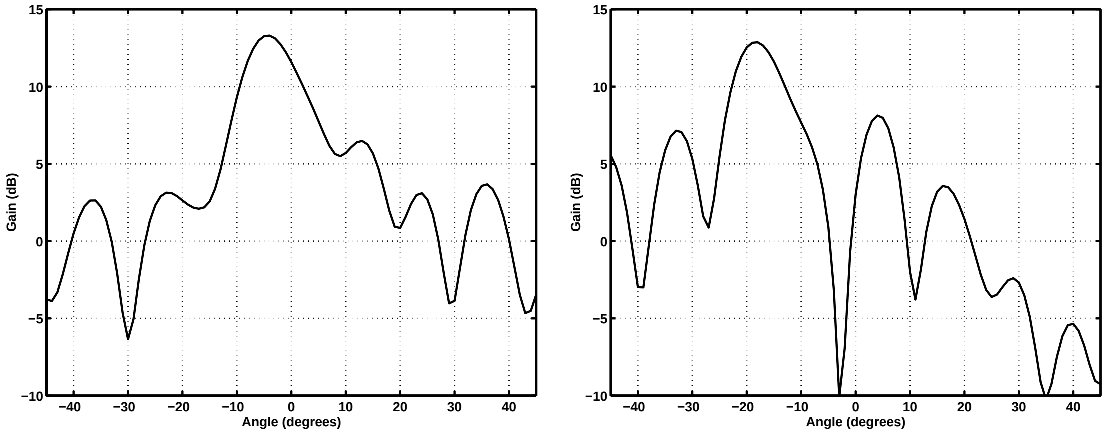

(a) Gain (dB) vs Angle of 0° beam port (b) Gain (dB) vs Angle of 20° beam port

Fig. 6. Results of Electromagnetic simulation

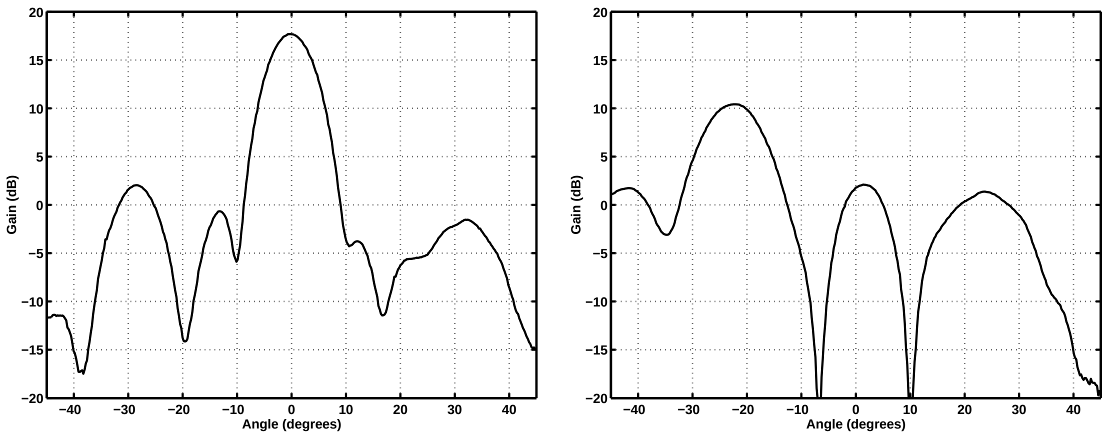

(a) Gain (dB) vs Angle of 0° beam port (b) Gain (dB) vs Angle of 20° beam port

Fig. 7. Measured performance of Rotman lens

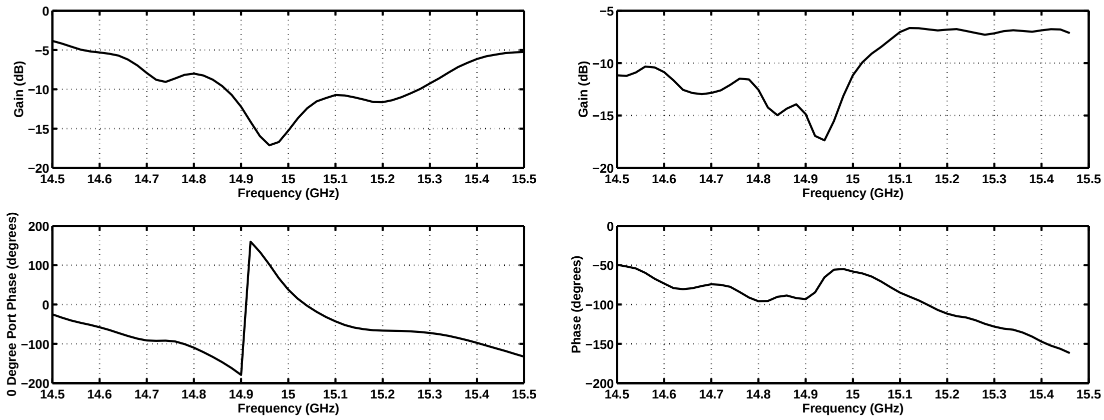

(a) Gain (dB) vs Angle of 0° beam port (b) Gain (dB) vs Angle of 20° beam port

Fig. 8. S_{11} of 0° and 20° ports

There is still a large discrepancy between the peak gain suggested by the numerical results (28 dB) and the measured results (17.5 dB). Radiation losses through the system arise from dissipation into the substrate. This is in the form of surface wave propagation, interactions at the input microstrip-to-lens transitions, spillover and aberrations within the lens system, interactions at lens-microstrip output feeds and will account for some of the lost gain. The majority of the lost gain is probably due to sidelobes outside the measured region and back radiation.

5. IMPROVEMENTS TO DESIGN

The Rotman lens described is the first 15 GHz prototype. Successive designs feature dummy ports along the sides of the Rotman lens to reduce reflections within the body of the lens. Much work has been done to improve the performance of the antenna and beam ports, improving bandwidth and reducing S_{11}.

The electromagnetic simulation of the successive designs promise greatly improved performance. Maximum gain and sidelobe levels are most noticeably improved but bandwidth and efficiency are still being developed.

Microstrip designs have been used because they are cheaper to manufacture and simpler than stripline to design. The increased difficulty of stripline designs is due to the requirement of aperture coupled patch antenna and the design of stripline to microstrip transitions or E-plane probes to connect the beamports to external devices. The lessons learnt using microstrip based lens design are directly applicable to stripline designs. Stripline designs offer the advantage of more compact design and greatly reduced radiation loss.

6. EXTENSION TO MM-WAVELENGTHS

A very convenient property of antennas is that its design frequency may be increase by simply scaling the antenna down. A Rotman lens with a fifteen element array designed using stripline techniques will require a substrate size of 60 mm by 60 mm at 37 GHz and 25 mm by 25 mm at 94 GHz. The by using 0.24 mm R5880 we can design 37 GHz lens using the same techniques as discussed above. To produce designs of substantially higher frequencies, the substrate thickness and minimum feature size becomes inhibitive. To overcome this problem, manufacturing using silicon or sapphire may be the solution. Although expensive, these techniques offer potentially very small substrate thickness and feature sizes necessary for frequencies of 94 GHz and beyond.

7. CONCLUSION

The design of Rotman lenses at mm-wavelengths has many challenges for the designer. This paper has demonstrated the potential for a Rotman lens at 37 GHz and the process a designer must go through to produce such a lens.

ACKNOWLEDGMENTS

This research is supported by funding from the ARC, the DSTO RF Hub, and the Sir Ross & Sir Keith Smith Fund.

REFERENCES

1. N. C. Currie and C. E. Brown, eds., *Principles and Applications of millimeter-wave radar*, Artech House, 1987.
2. T. Ihara, T. Manabe, M.Fujita, T. Matsui, and Y. Sugimoto, "Research activities on millimeter-wave indoor wireless communication systems at crl," *1995 Fourth IEEE International Conference on Universal Personal Communications* , pp. 197–200, 1995.
3. T. Ihara, Y. Sugimoto, and M. Fjita, "Research and development project for millimeter-wave premises communication systems," *Review of the Communications Research Laboratory* **41**(3), pp. 219–229, 1995.
4. L. O. Boric, Y. Nikawa, W. Snyder, J. Lin, and K. Mizuno, "Novel microwave and millimeter-wave biomedical applications," *4th International Conference on Telecommunications in Modern Satellite, Cable and Broadcasting Services. TELSIKS'99* **1**, pp. 186–193, 1999.
5. O. V. Betskii, N. D. Devyatkov, and V. V. Kislov, "Low intensity millimeter waves in medicine and biology," *Critical Reviews in Biomedical Engineering* **28**(1-2), pp. 247–268, 2000.
6. A. Mohamed, A. Campbell, D. Goodfellow, D. Abbott, H. Hansen, and K. Harvey, "Integrated millimetre wave antenna for early warning detection," in *Proc. SPIE Design, Characterization and Packaging for MEMS and Microelectronics*, pp. 461–469, October 1999.
7. D. Abbott, A. Moini, A. Yakovleff, X. T. Nguyen, A. Blanksby, G. Kim, A. Bouzerdoum, R. E. Bogner, and K. Eshraghian, "A new vlsi smart sensor for collision avoidance inspired by insect vision," *Proc. SPIE Intelligent Vehicle highway Systems* **2344**, pp. 105–115, November 1995.
8. D. Goodfellow, G. P. Harmer, and D. Abbott, "mm-wave collision avoidance sensors: future directions," *Proc. SPIE Sensing and Controls with Intelligent Transportation Systems* **3525**, pp. 352–362, November 1998.
9. D. Abbott, A. Bouzerdoum, and K. Eshraghian, "Two-dimensional smart arrays for collision avoidance," *Proc. SPIE Transportation sensors: Collision Avoidance, Traffic Management and ITS* **3207**, pp. 36–39, October 1998.
10. X. Nguyen, A. Bouzerdoum, R. Bogner, K. Eshraghian, D. Abbott, and A. Moini, "The stair-step tracking algorithm for velocity estimation," *ANZIIS-93* , pp. 412–416, December 1994.
11. A. Yakovleff, D. Abbott, X. T. Nguyen, and K. Eshraghian, "Obstacle avoidance and motion-induced navigation," *CAMP 95 Computer Architectures for Machine Perception Workshop* , pp. 384–393, 1995.
12. K. Chin and D. Abbott, "Motion detection using colour templates," *Proc. SPIE Design, Characterization and Packaging for MEMS and Microelectronics* , pp. 314–323, October 1999.
13. D. C. Goodfellow and D. Abbott, "Collision avoidance for nanosatellite clusters using millimeter-wave radiometric motion sensors," *Proc. SPIE Electronics and Structures for MEMS* **3891**, pp. 276–284, October 1999.
14. D. Abbott, A.Moini, A. Yakovleff, X. Nguyen, R. Beare, W. Kim, A.Bouzerdoum, R. E. Bogner, and K. Eshraghian, "Status of recent developments in collision avoidance using motion detectors based on insect vision," *Proc. SPIE Transportation Sensors and Controls* **2902**, pp. 242–247, November 1997.
15. A. Moini, A. Bouzerdoum, A. Yakovleff, D. Abbott, O. Kim, K. Eshraghian, and R. E. Bogner, "An analog implementation of early visual processing in insects," *International Symposium on VLSI Technology, Systems, and Applications* , pp. 283–287, May 1993.
16. X. T. Nguyen, K. Eshraghian, M. Moini, A. Bouzerdoum, A. Yakofleff, D. Abbott, and R. E. Bogner, "An implementation of smart visual micro-sensor based upon insect vision," *Proc.12 th Aust. Micro. Conf. Microelectronics, Meeting the Needs of Modern Technology* , pp. 129–134, October 1993.
17. A. Moini, A. Bouzerdoum, K. Eshraghian, A. Yakovleff, X. T. Nguyen, A. Blanksby, R. Beare, D. Abbott, , and R. E. Bogner, "An insect vision-based motion detection chip," *IEEE JSSC* **32**, pp. 279–284, Febuary 1997.
18. D. Abbott, A. Yakovleff, A. Moini, X. T. Nguyen, A. Blanksby, R. Beare, A. S. Beaumont, G. Kim, A. Bouzerdoum, R. E. Bogner, and K. Eshraghain, "Biologically inspired obstacle avoidance - a technology independent paradigm," *Proc. SPIE Mobile Robots X* **2591**, pp. 2–12, October 1995.
19. D. Abbott and A. Parfitt, "Collision avoidance device using passive millimetre-wave array based on insect vision," in *Proc. IREE 14th Australian Microelectronics Conference (Micro' 97)*, pp. 201–204, October 1997.
20. D. Abbott and A. J. Parfitt, "Extension of the insect-vision paradigm to millimeter waves," *Proc. SPIE Transportation Sensors* **3207**, pp. 103–106, October 1998.

21. D. Abbott, A. Bouzerdoum, and K. Eshraghian, "Future directions for motion detection based on the parallel computational intelligence of insects," *Proc. 23rd Euromicro Conference New Frontiers of Information Technology Short Contributions* , pp. 244–249, September 1997.
22. W. Rotman and R. F. Turner, "Wide angle microwave lens for line source applications," *IEEE Trans. Antennas Propagate* **AP-11**, pp. 623–632, November 1963.
23. J. Preissner, "The influence of the atmosphere on passive radiometric measurements," *Millimeter and Submillimeter Wave Propagation and Circuits* , pp. 48/1–14, 1979.
24. R. C. Hansen, "Design trades for rotman lenses," *IEEE Trans. Antennas Propagate* **39**, pp. 464–472, April 1991.
25. A. Balanis, *Microwave Engineering*, Harper and Row, 1982.
26. L. Hall, H. Hansen, and D. Abbott, "Design and simulation of a high efficiency rotman lens for mm-wave collision avoidance sensor," *Proc. SPIE Smart Electronics and MEMS* **4304**, December 2000.
27. K. K. Chan, "Planar waveguide model of rotman lens," *1989 IEEE AP-S International Symposium* **2**, pp. 651–654, June 1989.
28. M. Michaelides, "Microstrip transmission lines: impedance matching, coupling and filtering," *Mullard Technical communications* , pp. 170–176, October 1972.